ELSEVIER

International Journal of Mass Spectrometry 220 (2002) 127–136

International Journal of Mass Spectrometry

www.elsevier.com/locate/ijms

Rydberg Matter of K and N_2: angular dependence of the time-of-flight for neutral and ionized clusters formed in Coulomb explosions

Shahriar Badiei, Leif Holmlid*

Reaction Dynamics Group, Department of Chemistry, Göteborg University, SE-412 96 Göteborg, Sweden

Received 27 September 2001; accepted 21 March 2002

Abstract

Laser fragmentation via Coulomb explosions in a cloud of Rydberg Matter (RM) is shown to give an angular dependence of the time-of-flight (TOF) observations for neutral RM clusters. The RM cloud is formed by emission from a K doped FeO catalyst sample at 700–900 K and is formed of K^* atoms, or N_2^* molecules after nitrogen gas adsorption in the emitter. Close to the surface normal of the emitter, relatively large clusters from high excitation states in the RM dominate, while at large angles (40–50°) smaller clusters and monomers with high kinetic energy release from lower excitation states are observed more frequently. N_2 RM usually gives smaller clusters and more monomers than K RM. The extension of the RM cloud in the apparatus is easily observed by the different TOFs for the various particles at different angular settings of the detector, and by direct shifting of the laser focus point. The TOF results show well defined Rydberg states and RM clusters with very low translational temperature, below 100 K even for the monomers. (Int J Mass Spectrom 220 (2002) 127–136)

Keywords: Rydberg Matter; Coulomb explosions; Clusters; Time-of-flight; Rydberg states

1. Introduction

The electronically excited condensed phase named Rydberg Matter (RM) can be formed rather easily by condensation of circular Rydberg states of alkali atoms [1,2]. Recently, Rydberg states of H_2 and also RM clusters were shown to be formed from a K promoted catalyst sample [3,4]. Raman studies identify both alkali Rydberg states [5] and electronic transitions in RM [6] at RM emitter surfaces. It is also possible to form RM from N_2 gas, as shown by stimulated Raman studies in the IR [7]. Laser fragmentation coupled to time-of-flight (TOF) measurements of ions and neutrals has identified the size and form of K RM clusters [8,9]. We now apply the neutral TOF method to the study of the RM cloud formed by K and N_2 outside a K promoted iron oxide catalyst. The very similar angular variation at short TOFs for K and N_2 is of special significance, since it shows that the laser fragmentation pattern changes with angle in a well specified manner.

2. Theory

The most important route to RM formation from H_2 and N_2 molecules starts with thermal desorption of circular Rydberg states of alkali metal from surfaces [10] which gives facile condensation to RM clusters in

* Corresponding author. E-mail: holmlid@phc.gu.se

1387-3806/02/$ – see front matter
PII S1387-3806(02)00689-9

the boundary layer of the surface. K Rydberg atoms at surfaces form Rydberg clusters in the surface sheath bound to the surface [11]. Direct spectroscopic observations of the excited alkali atoms in the surface boundary layer at the emitter surface by stimulated anti-Stokes Raman scattering are possible [5]. Excited clusters of alkali atoms with long radiative lifetimes are observed in desorption [12,13]. In subsequent collisions of desorbing alkali Rydberg atoms and clusters with gas atoms and molecules just outside the emitter, probably in the emitter boundary layer, transfer of excitation energy is possible. In studies of energy transfer from Cs Rydberg species to molecules like H_2 and N_2 giving molecular ions, it was concluded that Rydberg clusters were involved [2,14]. The desorbing RM clusters may act as condensation nuclei, giving the rapid condensation observed. This type of mechanism was studied for $K_N + K$ cluster condensation [13]. Similar processes were also studied [11,15]. Recently, a similar cluster condensation process was reported by Peng et al. [16]. In a theoretical study, highly excited polar Rydberg dimers of alkali atoms were predicted [17]. Such polar dimers could act as very efficient condensation nuclei in the boundary layer at the surface, as well as in the gas phase. Thus, there are several possible pathways for the transfer of thermal excitation energy from the surface to the observed RM clusters consisting of gas molecules, via Rydberg alkali atoms, Rydberg alkali dimers and Rydberg alkali clusters to Rydberg molecules forming the RM clusters.

The RM clusters form a cloud around the emitter, of a very low density. In this cloud, the clusters are bound together by links to other clusters, which makes them almost fixed in space. Thus, the region at the laser focus is depleted of RM material after a few minutes. According to theory [18], a bonding in the RM can only exist if all atoms or molecules in the RM have the same excitation state. It is also apparent that the electronic excitation energy will be equally divided between all atoms or molecules in the RM, since the electrons are delocalized and will move over even macroscopic distances. Thus, if a ground state species is incorporated into the RM structure, it will share the excitation energy with the other species in the RM. The atoms or molecules in the RM are in a condensed matter and have lost their initial Rydberg electron to the conduction band. When the laser pulse interacts with the RM, the electrons are displaced, or seen in another way, excited into higher states in the conduction band. As in the more usual case with delocalized electrons in molecules, such higher states may not surround or cover all atoms/molecules in the RM. Thus, it is possible that the laser pulse with its high electric field excites the electrons responsible for the bond between two clusters (two corner atoms) to make this point in the structure uncovered by the electron cloud. In such a case, a Coulomb repulsion between the two naked ions may rip away a small cluster from the large and heavy, otherwise intact cloud. The cluster released will be neutral, but with a polarized electron cloud. After some time, this cloud will relax back to lower states covering or surrounding all atoms in the cluster, but by that time the cluster released may be far away from the repelling charge.

The Coulomb interaction between two positive charges suddenly formed at a distance d is a repulsion that forces the charges apart. The total kinetic energy transferred to the relative motion between the two separating charges is equal to the Coulombic energy

$$W = \frac{e^2}{4\pi\varepsilon_0 d} \tag{1}$$

where e is the elementary charge and ε_0 is the vacuum permittivity. The TOF for the particles released by such Coulomb explosions is calculated with $d = 2.9n^2a_0$, where a_0 is the Bohr radius. Both the classical and QM calculations for RM give a simple relation between the excitation level of RM and the bond distances between the core ions in the RM. The factor 2.9 is found from the classical calculations of the minimum energy states of RM [18]. The TOF is then found from $t = s/(v + v_0)$, where s is the distance to the detector, $v_0 = (2W/m)^{1/2}$, m is the cluster mass and v is a thermal initial velocity component. The probability distribution of $v_{tot} = v + v_0$ is

$$P(v_{tot}) \propto (v + v_0)^2 \exp\left(\frac{-mv^2}{2kT}\right) \tag{2}$$

with $T = T_{RM}/N$. Here, N is the number of monomers in the cluster. T_{RM} is the actual macroscopic temperature of the RM cloud surrounding the emitter in the experiments. The factor $(v+v_0)^2$ means that a density velocity distribution is used, since this distribution corresponds to the initial stationary cloud.

When a distribution of the form $P(v)$ matches a narrow experimental cluster TOF peak, it is possible to extract a temperature T for the thermal initial motion of the clusters, the cluster size N, the energy release W and from this also the ion–ion distance d at the start of the Coulomb explosion, and the corresponding principal quantum number n. The energy spread due to thermal initial energy prevents the observation of the small kinetic energy release from Coulomb explosions with $n > 10$. Experiments using Coulomb explosions with K RM clusters give bond distances of 4 nm from the observed excess energy of 0.38 eV [9], corresponding to $n = 5$.

3. Experimental

The experiments are carried out in an UHV apparatus with a base pressure of 1×10^{-8} mbar. It has been fully described previously [13]. A schematic picture of the setup is shown in Fig. 1. In the N_2 experiments, a laser dump was placed inside the vacuum chamber. In the K experiments, the dump was outside a window, and the detector was improved (see in the following description). The commercial iron oxide catalyst sample is placed slightly behind the center of the UHV chamber. It is folded in a thin Ta foil with a flat surface cut in the exposed part. An AC heating current of <30 A was fed through the Ta foil to heat the sample, so it emits RM particles. The emitter is held in the vertical direction by two current conducting arms, and the current flows through the emitter (the Ta foil) in the vertical direction. The 50 Hz AC current used with the 10 Hz repetition of the laser pulse means that any magnetic or electric field (from the 0.8 V drop over the emitter) influence is averaged out in the final TOF distributions. Of course, the neutral flux studied is not in any way deflected by the electric field. The emitter initially contains 8 mol% K and is used in large scale production of styrene from ethyl benzene in the chemical industry [19,20]. It is normally heated to 700–900 K during the experiments (interpolated from pyrometric data). The heating of the emitter is necessary to increase the diffusion rate of the K atoms and the adsorbed gas molecules in the porous emitter.

A Nd:YAG pumped dye laser (Lambda-Physik) gives 5 ns pulses at a maximum average power at the UHV chamber of 200 mW with a repetition rate of

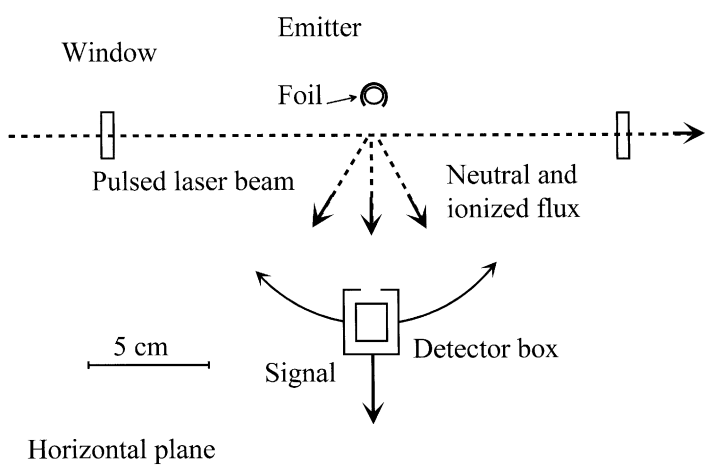

Fig. 1. Schematic diagram of apparatus used in the K cluster experiments. Horizontal cut. The detector is mounted in a rotatable lid in the vacuum chamber.

10 Hz. Normally, the laser is tuned to 564 nm at the maximum intensity of the Rhodamine 6G dye. A single lens with a focal length of 0.4 m is used to focus the laser beam. The beam enters through a window in the vacuum chamber and passes very close to the center of the chamber, at a distance of 5–15 mm in front of the emitter surface. The plane of polarization is in the vertical direction, perpendicular to the laser beam–detector plane. The detector can be rotated around the emitter and its opening is placed 8.2 cm from the emitter. The only particles which can be measured by the detector are Rydberg states that can become field ionized in the detector to give positive ions, and positive ions when an accelerating field for ions exists between the emitter and the detector. Two different detectors have been used, but with the same shape of the field ionization and ion entrance part. The ions formed in (or entering) the detector are drawn either into a channel electron multiplier (CEM) or onto a Cu–Be dynode, which is part of a dynode–scintillator–photo multiplier chain [21]. The effective TOF path ends at the point of ionization or ion deflection inside the detector housing. The resulting pulses are further amplified and measured by a multi-channel analyzer (MCA). Due to the formation of a cloud of RM around the sample, the flight path may be shorter to the detector at large detector angles. This is shown in Fig. 2.

In the experiments, a cloud of RM is formed in the UHV apparatus by mild heating of the iron oxide catalyst emitter. This cloud will probably be quite fractal in nature, and its filling factor (actual volume of RM relative to the total volume containing RM) will probably be rather low. The laser pulses release clusters from the region outside the emitter. In most of the experiments described as follows, neutral clusters are detected. If they only had thermal energies, their TOF peak widths would be very large, of the order of milliseconds, and no time resolution would be obtained in the spectra. In Fig. 3, the low, broad curve corresponds to neutral K* with no kinetic energy release (KER), but only with an initial 200 K thermal kinetic energy distribution. The fact that the clusters arrive much faster and with well defined TOF peaks proves

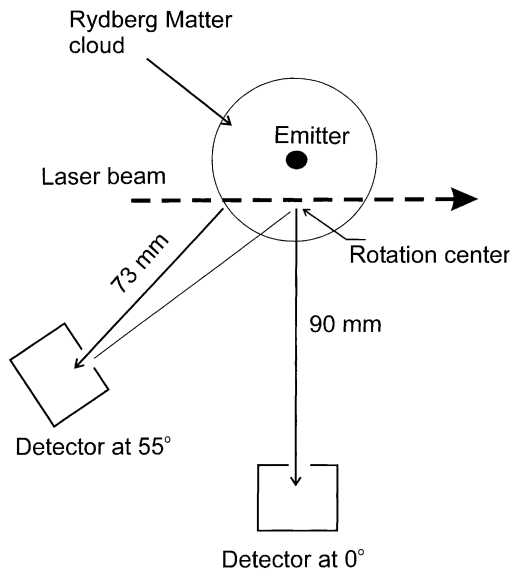

Fig. 2. The cloud of RM gives a short effective flight path for the signal obtained at large angles. The cloud here has a radius of 24 mm, which gives the flight distances 73 and 90 mm in agreement with fits to the experimental TOF peaks.

that they have received a well defined excess energy (KER) from the laser fragmentation (Coulomb explosion) process. The sharp peaks in Fig. 3 correspond to translationally excited species with KER of 0.59 eV, starting with a thermal distribution of $200/N$ K [4]. A quick glance at the experimental results for K_N^* shows

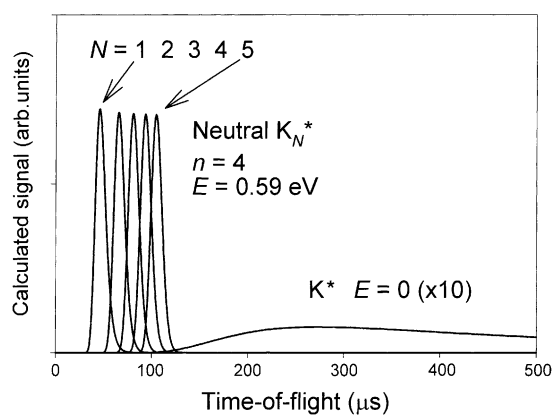

Fig. 3. Simulated distributions for a temperature $T = 200/N$ K, where N is the number of monomers in the cluster. The sharp peaks have KER, while the slow peak has only thermal energy (cf. the experimental results shown in the following figures).

the similarity between these fast peaks and the experimentally observed peaks.

By using a relatively low temperature of the emitter, approximately 700 K, it is possible to obtain a K RM cluster signal also from a fresh emitter and with no gas admission. After a few hours, the K signal decreases but it can be restored by small shifts of the position of the laser beam, or by just cutting off the laser beam for an hour or so. Thus, the signal loss is due to depletion of K in the RM cloud. When nitrogen gas is leaked into the vacuum chamber giving a pressure of 5×10^{-6} mbar for 1 h or more, usually at higher temperature, TOF peaks are observed due to adsorption of gas in the porous emitter and subsequent excitation and condensation of the Rydberg molecules. After some time, the gas TOF peaks disappear slowly. The entire process is repeated after renewed gas admission. The TOF results presented here are all obtained after pump-out to a pressure less than 1×10^{-8} mbar.

4. Results and discussion

In the present study, we concentrate on laser fragmentation studies of a cloud of RM using angular resolved TOF spectra. Both neutral clusters K_N^* and $(N_2)_N^*$ as well as ionized clusters K_N^+ are studied.

4.1. Low energy K_N^+ ions

Typical results with no adsorbed gas in the emitter, thus with only K clusters, are shown in Fig. 4 for the signal observed in the direction of the surface normal. The variation of the TOF spectra with applied voltage is strong. Ions are primarily observed in the TOF range 150–500 μs, and neutrals are observed at shorter times. This is easily observed, since the ions are accelerated by the increased voltage but the neutrals are largely unchanged in TOF position. The broad peak at the longest TOF is so slow that it corresponds to a heavy cluster. The cluster $N = 37$ observed previously [8] should take slightly longer time to the detector. Assuming a low KER of 0.1 eV in the laser fragmentation process due to the Coulomb explosions, good agreement is found for $N = 37$. This KER corresponds to an excitation state of $n > 8$. The ion clusters observed with 10 V acceleration seems to be $N = 7$, 14, and 37 (from two different states for the two last peaks). The first of the $N = 37$ peaks corresponds to a KER of

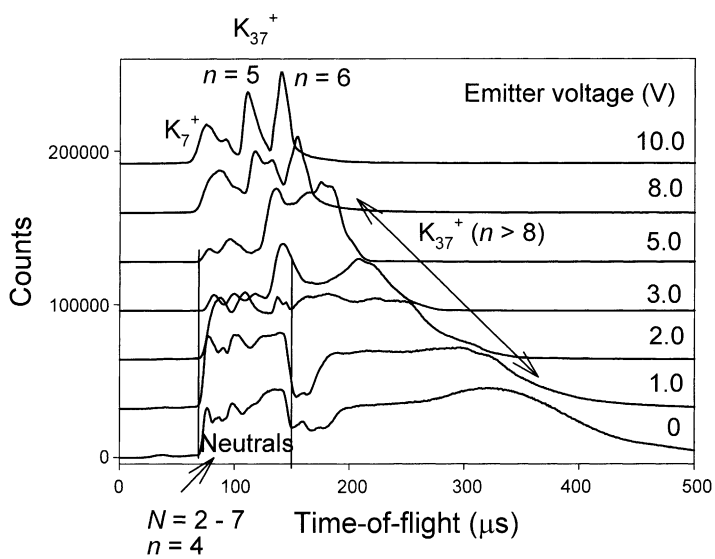

Fig. 4. TOF spectra for K RM clusters at 0°, the direction of the surface normal. The emitter voltage is indicated. At low voltage, the light K_N^* clusters, $N = 2$–7, do not ionize but retain their neutral TOF. To the right, heavy K_N^+ clusters are accelerated by the field.

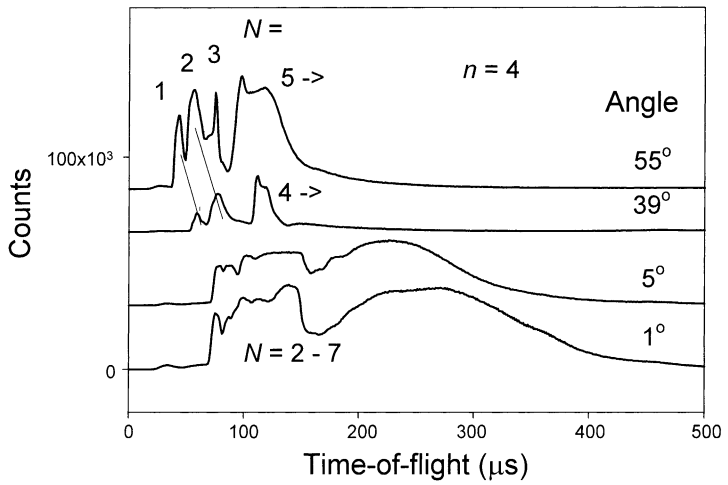

Fig. 5. TOF spectra for neutral K clusters, at ground potential of the emitter and a few different angles. The lightest clusters are assigned. The excitation state is $n = 4$. The best fit is found for flight distances of 90 mm (equal to design) for 1° and 5°, 97 mm for 39°, and 73 mm for 55°.

0.35 eV and, thus, to $n = 5$, while the second corresponds to a KER of 0.1 eV and less well defined values of $n > 8$. Thus, large K RM clusters are observed as peaks and not only as depletion dips as previously [8].

4.2. No small K_N^+ ions

It is interesting to observe that the flux due to ions K_N^+ with only a few atoms, i.e., low N is small. No atomic K ions or dimer ions are observed. In Figs. 4 and 5 it is shown that the neutral dimer K_2^* is the first TOF peak at small angles with zero voltage on the emitter, but no corresponding ion peak is observed. Other small neutral clusters are also observed with $N = 3$–6, but no ions with such small N values are seen in the TOF spectra. In general, it is expected that ions should be formed from the neutral clusters, if the clusters could be ionized by the laser. In the present case, no such small ions are observed and the conclusion is that the clusters are not ionized by the laser. This is in agreement with the description of the laser excitation process given in Section 2. Instead, neutral clusters are released by the laser as described there, and these clusters may then be field ionized in the static electric field, if a strong field is applied.

The reason why such cluster ions are not observed here may be that they are not stable. In the case of RM clusters with large interionic distances, ionization of a small cluster will change its stability strongly. The electron density on the small ionized RM clusters will probably be too low to keep the cluster stable. The ion fragments formed by the decomposing clusters will move in a cone around the parent cluster direction, and may not be detectable with small emitter potentials. Another possibility is that the ions and their neutral precursors move even initially in directions outside the detector plane. This is supported by the results in [9], where small K ion clusters are observed by rotating the plane of polarization of the laser to the horizontal direction. This apparently brings the initial KER in the detector plane, which makes the ions detectable.

4.3. Directed flux of neutral clusters K_N^*

Another important observation can be made from Figs. 4 and 5, namely that neutral clusters K_N^* with large values of N (flight times at 300 μs or so) are not observed at large angles from the emitter normal. At 0 V in Fig. 5, no large clusters are observed at large angles. (However, when the emitter voltage is increased at large angles, an intensity at long flight times

appears due to ions.) This implies that the KER of 0.1 eV derived earlier is directed in space, almost perpendicular to the laser beam. With an accelerating voltage, the large cluster ions are drawn out in all directions due to the circular symmetry of the apparatus, but the neutral large clusters (or ionized clusters in zero field) only translate in a direction roughly perpendicular to the laser beam. This observation is clearly compatible with an ordered structure of the clusters in the RM cloud, and most likely corresponds a structure where the planar clusters are lined up perpendicular to the laser beam. This structural ordering could possibly be due to the strong magnetic interaction between the clusters, caused by their large magnetic dipole moments [18].

4.4. High energy neutrals K_N^*

The results in Figs. 4 and 5 also show the behavior of the neutral clusters at zero volts accelerating potential. At small angles from the normal direction of the surface, neutral clusters with $N = 2$–7 and excitation state $n = 4$ are observed. At large angles, the cluster signal arrives so early that a good fit can only be found assuming that also monomers K* are released with an energy of 0.59 eV corresponding to $n = 4$. This point is supported strongly by the angular distribution in Fig. 6. The obvious shift in the figure of the first rising edge at 15° relative to the 0° direction is apparently already due to a monomer contribution. The gradual shortening at even larger

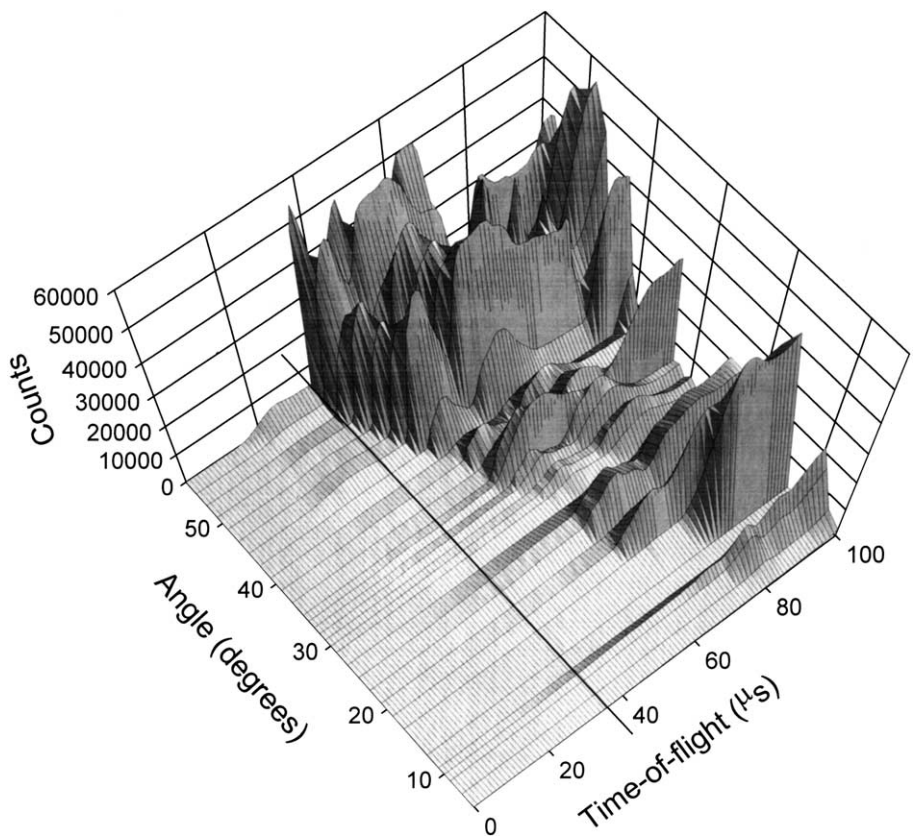

Fig. 6. Angular variation of the TOF spectra for neutral K clusters, at flight times up to 100 μs. The signal height appears to vary with angle, since the RM cloud disappears slowly with time during the runs, probably due to depletion of K in the covalent state on the emitter surface. Note that the shortest TOF changes strongly with angle (cf. Fig. 5).

angles is mainly due to a shortening of the effective flight distance by the size of the RM cloud (see Fig. 2 and the following description).

4.5. High energy neutrals $(N_2)^*_N$

The angular variation of the TOF spectra for $(N_2)^*_N$ clusters is interpreted by detailed calculations in Fig. 7. In Fig. 8, the results are shown as a three-dimensional plot similar to the K cluster results in Fig. 6. Both Figs. 7 and 8 show that close to the surface normal, longer flight times are found, while at larger angles, shorter times and even two different ridges on the distribution are observed. The calculated peaks in Fig. 7 show that a pattern of monomers N_2^* and dimers $(N_2)_2^*$ with two different KER values, with $n = 4$ at small angles and $n = 3$ at large angles describes the experimental results well. This result is based both on the width of the peaks and on their TOF positions. Since K^* cannot be in the $n = 3$ state in the RM, the TOF observed are much too short to correspond to K. Thus, the interpretation as N_2 states is certain. In the case of N_2 clusters, the complete TOF spectra are interpreted as shown in Fig. 7. Peaks from different excitation states do coexist at intermediate angles. This has not been observed with certainty before.

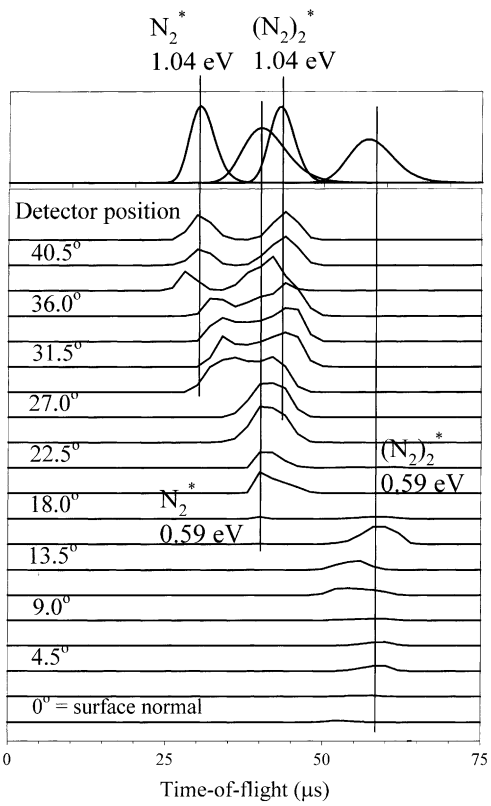

Fig. 7. Neutral TOF spectra for N_2 molecules and clusters with calculated spectrum at top. Close to the normal, a lower value of the KER is found, corresponding to $n = 4$. At larger angles, $n = 3$ is found instead. Note that K cannot be in $n = 3$ Rydberg states, and that the TOF is too short to correspond to K^*.

The formation of dimers of N_2 is a remarkable feature in the experiments, since the equilibrium vapor pressure of nitrogen gas at room temperature is much too high to give any cluster formation from ground state molecules. Observations of clusters under high temperature and low pressure conditions are coupled to formation of Rydberg states [22,23]. The long-range bonding attraction [18] in the RM gives cluster formation also under low density conditions.

4.6. RM cloud size observed

The angular variation is at least partially explained by the size of the RM cloud around the emitter. This means that the particles released from the cloud in the direction of the surface normal come from the inner, denser region close to the emitter, since the laser beam passes through this region. At larger angles, the particles come from a region further out which is less dense, apparently giving more monomers and smaller clusters. The extension of the RM cloud is also partly the cause of the shorter flight times at larger angles observed in Figs. 6 and 8. At large angles, the laser passes though the RM cloud at a larger distance from the emitter, and thus closer to the detector when it is rotated to such angles. This is shown in Fig. 2, where the results for the flight distances from Fig. 5 are reproduced. The difference in the angular ranges observed for the two different values of KER for N_2 clusters is obviously due to a more dynamic effect in the laser fragmentation process, which requires further studies.

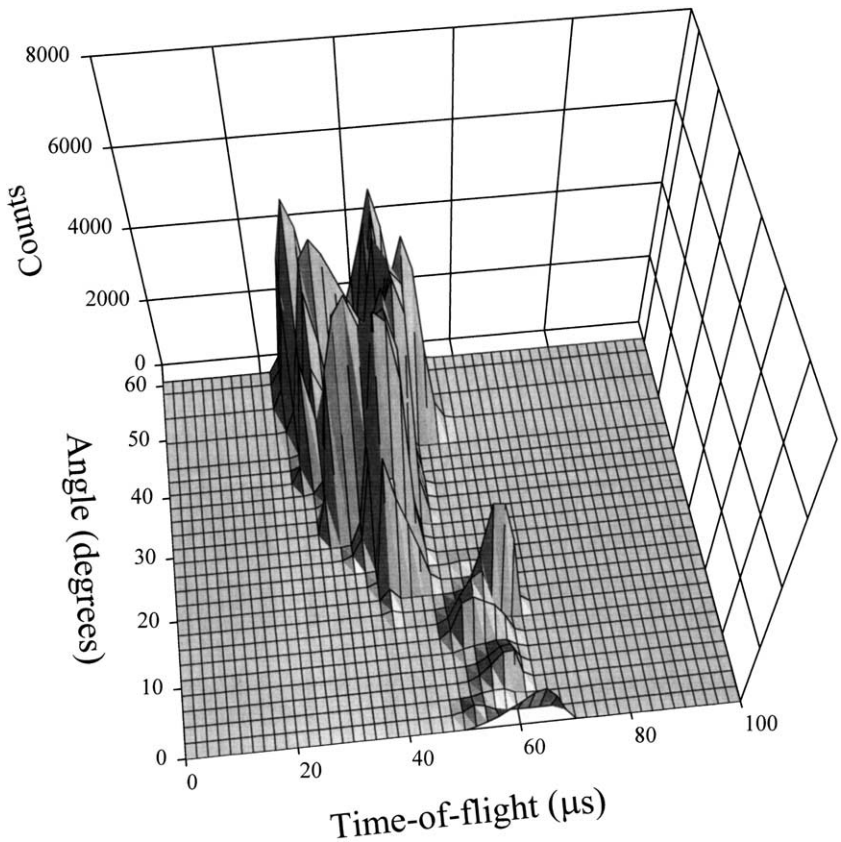

Fig. 8. Combined angle–TOF neutral particle spectra with pre-adsorbed N_2. At the surface normal at 0° a low intensity peak is observed, while at large angles from the surface normal, higher intensity peaks at short flight times are seen. Note that the TOF decreases for larger angles for the same peak (cf. Figs. 6 and 7).

The existence of the RM cloud is also easily observed by moving the focusing lens along the laser beam with the detector at a large angle relative to the normal of the surface. In this way, it is seen that with the focus point closer to the detector, the TOF becomes shorter. Thus, the extension of the RM cloud is observed directly. There are several facts that exclude that a plasma is formed around the emitter, instead of an RM cloud. With a plasma, a continuous background signal is expected, especially when the emitter is at positive voltage, and no such signal is observed. There is no shift in the behavior in Fig. 4, for example, when the voltage is shifting from zero to positive, which would also be expected in the case of free charges in a plasma. That a plasma should release neutral K_N^* clusters due to the laser pulse, is of course, not possible. That such clusters would have well defined kinetic energies, is of course, absolutely at variance with the chaotic nature of a plasma. Thus, that plasma formation could be the reason for the results presented here can, thus, be safely rejected.

The temperature of the N_2 monomers in the calculation in Fig. 7 is 100 K, thus much lower than the temperature of the surrounding apparatus, including the hot emitter. Even lower translational temperatures can be found for H_2 [4] and K [24] clusters. The low kinetic temperature observed is probably due to cooling of the RM by electron emission. A more complete treatment of this has recently been submitted.

5. Conclusions

Laser fragmentation TOF observations via Coulomb explosions in a cloud of RM are shown to give results that vary with angle around the emitter and the laser beam. Close to the surface normal, relatively large clusters from high excitation states in the RM dominate, while at large angles (40–50°) smaller clusters and monomers with high KER from lower excitation states are preferentially observed. This is true both for K and N_2 RM, but N_2 usually gives smaller clusters and more monomers than K. The extension of the RM cloud in the apparatus is easily observed by the different TOFs for the various particles at different angular settings of the detector, and by direct shifts of the laser focus point. The TOF results show well defined Rydberg states and RM clusters with very low translational temperature, well below 100 K even for the monomers.

Acknowledgements

The support from the Swedish Research Council for Engineering Sciences (TFR) is gratefully acknowledged.

References

[1] R. Svensson, L. Holmlid, Surf. Sci. 269/270 (1992) 695.
[2] R. Svensson, L. Holmlid, Phys. Rev. Lett. 83 (1999) 1739.
[3] J. Wang, L. Holmlid, Chem. Phys. 261 (2000) 481.
[4] J. Wang, L. Holmlid, Chem. Phys. 277 (2002) 201.
[5] L. Holmlid, Langmuir 17 (2001) 268.
[6] L. Holmlid, Astrophys. J. 548 (2001) L249.
[7] L. Holmlid, Phys. Rev. A 63 (2001) 013817.
[8] J. Wang, L. Holmlid, Chem. Phys. Lett. 295 (1998) 500.
[9] J. Wang, L. Holmlid, Chem. Phys. Lett. 325 (2000) 264.
[10] L. Holmlid, J. Phys. Chem. A 102 (1998) 10636.
[11] J. Wang, K. Engvall, L. Holmlid, J. Chem. Phys. 110 (1999) 1212.
[12] J. Wang, L. Holmlid, Surf. Sci. 425 (1999) 81.
[13] A. Kotarba, K. Engvall, J.B.C. Pettersson, M. Svanberg, L. Holmlid, Surf. Sci. 342 (1995) 327.
[14] J. Lundin, L. Holmlid, J. Phys. Chem. 95 (1991) 1029.
[15] L. Holmlid, Z. Phys. D 34 (1995) 199.
[16] X. Peng, J.E. Abbott, W. Kong, J. Chem. Phys. 113 (2000) 3020.
[17] C.H. Greene, A.S. Dickinson, H.R. Sadeghpour, Phys. Rev. Lett. 85 (2000) 2458.
[18] L. Holmlid, Chem. Phys. 237 (1998) 11.
[19] G. Meima, P.G. Menon, Appl. Catal. A 212 (2001) 239.
[20] L. Holmlid, P.G. Menon, Appl. Catal. A 212 (2001) 247.
[21] L. Holmlid, B. Lönn, J.O. Olsson, Rev. Sci. Instrum. 52 (1981) 63.
[22] C. Åman, J.B.C. Pettersson, L. Holmlid, Chem. Phys. 147 (1990) 189.
[23] J. Wang, R. Andersson, L. Holmlid, Surf. Sci. 399 (1998) L337.
[24] S. Badiei, L. Holmlid, Chem. Phys., in press.